

# ESTIMATION OF ORIENTATION AND POSITION OF THE MANIPULATOR USING THE EXTENDED KALMAN FILTER BASED ON MEASUREMENTS FROM THE ACCELEROMETERS

Submitted: 6<sup>th</sup> February 2019; accepted 15<sup>th</sup> April 2019

Agnieszka Kobierska, Piotr Rakowski, Leszek Podśędkowski

DOI: 10.14313/JAMRIS/2-2019/15

## Abstract:

Authors present the kinematic structure of measurement arm along with its construction for efficient estimation of orientation and position of the manipulator using extended Kalman filter. The major innovation of the arm is that it only uses accelerometers as gravity sensors for determining relative positions of the links. This article presents the problem of position estimation based on measurements with high noise and the use of the extended Kalman filter to limit the impact of noise on the measurement. Repeatability tests were performed using custom made test stand.

**Keywords:** EKF, accelerometers, measuring arm

## 1. Introduction

Large industrial manipulators make use of optical encoders or resolvers to measure the angular position of the joints. The dimensions of these encoders or resolvers do not affect the operating of the manipulator. These sensors also do not restrict the movement of manipulator arm during operation. However, for special mini manipulators, finding a cost-efficient sensor of required dimension is a challenge. The manipulator used in this study is a disposable medical device used for measuring the change in length of the femoral bone before and after the hip replacement surgery. Hence, a low-cost sensor is required for accurate measurement.

Recently, accelerometers are being employed as cheaper alternatives to standard sensors for angular measurement [3][4][5][7]. In addition, the use of accelerometers reduces the overall components in the assembly, which makes the sterilization process easier. Our research is focused on obtaining accurate measurements. However, one of the major disadvantages of using accelerometers, in this application, is the lack of arbitrary positioning of the joint whose angular position needs to be determined. When the joint rotates around the vertical axis, the accelerometers are found to be incapable of detecting changes in the joint angle. However, rotation around the vertical axis can be avoided by developing an appropriate kinematic construction of the manipulator arm. This ensures continuity of angular measurement and the correct operating of the manipulator [2].

## 2. Position Estimation

The manipulator (measurement arm) with six degrees of freedom is based on the kinematics described by the Denavit–Hartenberg (D-H) notation. Table 1 defines the position of the tip (Link 6) of the arm with respect to the base of the arm (Link 0). The manipulator arm has no driving elements and is used for measurement in static position. The individual parts of the manipulator (Fig. 1) are connected by rotary joints with one degree of freedom.

**Tab. 1.** D-H notation of manipulator

Link name	Nr	$\theta_i$ ( $\theta_0$ )	$d_i$ [mm]	$a_i$ [mm]	$\alpha_i$
Link 1	1	$\theta_1$ (90°)	13	20	-90°
Link 2	2	$\theta_2$ (0°)	0	80	0°
Link 3	3	$\theta_3$ (0°)	19.25	5	-90°
Link 4	4	$\theta_4$ (0°)	100	-5	90°
Link 5	5	$\theta_5$ (90°)	24.25	20	-90°
Link 6	6	$\theta_6$ (90°)	0	0	45°

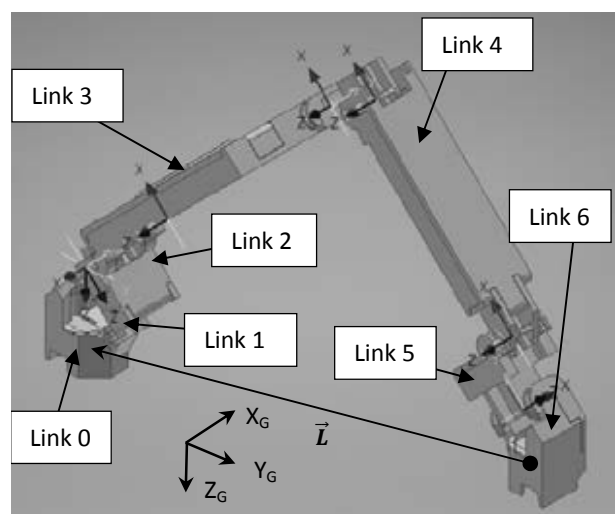


**Fig. 1.** The manipulator links connected by rotary joints

To determine the coordinates of the gravity vector in each link coordinate system and the angles of rotation of individual joints, accelerometers (type FXLS8471Q) are attached to each of the links (from 0 to 6).

The method used for measurement of angles using accelerometers is presented in [1]. The study also presents the possibility of achieving accurate measurements and indicates the directions for further improvements. This study presents the problem of position estimation based on measurements with noise and the use of extended Kalman filter (EKF) to limit the impact of noise on the measurement.

The state vector of the object (process) is called the minimum set of all internal variables whose knowledge at a given point of time together with the knowledge of future waveforms of input variables (when omitting nonmeasurable disturbance variables) allows unambiguous determination of future time courses of output variables [6].

In this study, the number of parameters (variables) describing the position of the tip in the base system is 6: (3 coordinates of positions:  $x, y, z$  and 3 coordinates of orientation: Roll (z-axis), Pitch (y-axis), Yaw (x-axis)). The dependence of the position of the tip relative to the base is determined by the vector  $L = [L_x, L_y, L_z]$ : from the center of the coordinate system of base up to the characteristic point on Link 6 ( ${}^6L = [L_{x6}, L_{y6}, L_{z6}]^T$ ). The orientation parameters are determined by the rotation matrix  $R$ , describing the orientation of the tip layout relative to the base. To completely describe the object's state in the global coordinate system, we still need to determine the location of its base, which similarly has 6 parameters: (3 coordinates of position:  $x, y, z$  and 3 coordinates of orientation: Roll (z-axis), Pitch (y-axis), Yaw (x-axis)). In case of the manipulator used in this study, only the two global parameters concerning the orientation are possible to determine: Roll (z-axis) and Pitch (y-axis).

Representation of the  $L$  vector in the base system (Link 0):

$${}^0\vec{L} = A_0^6 {}^6\vec{L}; {}^6\vec{L} = \begin{bmatrix} L_{x6} \\ L_{y6} \\ L_{z6} \\ 1 \end{bmatrix} \quad (1)$$

where  $A$ , matrix of transformations, according to the D-H notation, is equal to:

$$A_i = Rot_{(z,\theta_i)} Trans_{(z,d_i)} Trans_{(x,\alpha_i)} Rot_{(x,\alpha_i)} \quad (2)$$

$$A_i = \begin{bmatrix} c\theta_i & -s\theta_i c\alpha_i & s\theta_i s\alpha_i & a_i c\alpha_i \\ s\theta_i & c\theta_i c\alpha_i & -c\theta_i s\alpha_i & a_i s\alpha_i \\ 0 & s\alpha_i & c\alpha_i & d_i \\ 0 & 0 & 0 & 1 \end{bmatrix} \quad (3)$$

where  $c\theta_i$  or  $c\alpha_i$  – means cosine of the angle,  $s\theta_i$  or  $s\alpha_i$  – means sine of the angle. Matrix of transformation of the arm takes the following form:

$$A_0^6 = A_0^1 A_1^2 A_2^3 A_3^4 A_4^5 A_5^6 \quad (4)$$

and depends on the angles  $\theta_i$  in the manipulator joints:

$$A = f(\theta) \text{ with } \theta = [\theta_1, \dots, \theta_6]. \quad (5)$$

The coordinate system  $X_G, Y_G, Z_G$  was established in such a way that the axis  $Z_G$  of the gravity system was directed downwards, and the  $X_G$  axis coincided

with the projection of the axis of rotation of the joint to the level. Two angles  $\beta_y$  and  $\beta_z$  have been defined with the rotation of the system 0 in relation to the  $G$  system, where  $\beta_y$  determines the angle between the axes  $Z_G$  and  $Z_0$ , and  $\beta_z$  determines the angle between the axes  $Y_G$  and  $Y_0$ . The condition for the correct adoption of the gravity system is the implementation of the transformation of the gravitational acceleration version in the D-H system associated with the arm link meets in the form:

$$R_G^0(\beta_y, \beta_z) E_0 = \begin{bmatrix} 0 \\ 0 \\ 1 \end{bmatrix} \quad (6)$$

where:

$$R_G^0 = R_{y,\beta_y} R_{z,\beta_z} = \begin{bmatrix} c\beta_y c\beta_z & -c\beta_y s\beta_z & s\beta_y \\ s\beta_z & c\beta_z & 0 \\ -s\beta_y c\beta_z & s\beta_y s\beta_z & c\beta_y \end{bmatrix} \quad (7)$$

is the rotation matrix of the transition from the "0" system to the gravity system.

The static data obtained from the measurements are used to determine the estimated parameters of the system model. The data in the registered sample are only the measure of the real parameters with some errors. During data processing, the state of the system is estimated taking into account the measurement probability parameters (measurement noise, measurement system errors). The probability parameters of the estimation is also estimated.

With regards to the described manipulator, the estimation of the position depends on the accuracy of the accelerometers in measuring the individual variables  $\theta_i$  and angles  $\beta_y$  and  $\beta_z$ .

For this manipulator:

– The state vector is presented as:

$$X = [\theta_1, \theta_2, \theta_3, \theta_4, \theta_5, \theta_6, \beta_y, \beta_z]_{(8*1)}^T \quad (8)$$

– The exit vector as a measure of the acceleration direction:

$$Z = [E_0; E_1; E_2; E_3; E_4; E_5; E_6]_{(21*1)} \quad (9)$$

where  $E_i = [e_{x_i} \ e_{y_i} \ e_{z_i}]^T$  determines versors of the gravitational acceleration in a D-H coordinate frame coupled with the  $i$ -th link of the arm.

The dependence between the  $E_i$  versor and the readings from the accelerometer sensors has the form:

$$E_i = K_i \begin{bmatrix} a_{x_i} \\ a_{y_i} \\ a_{z_i} \\ 1 \end{bmatrix}, \quad (10)$$

where:  $K_i$  is the calibration matrix determined as in [1] taking into account the transition from the sensor system to the D-H system of the arm.

The output function  $h$  estimating the output vector based on the state variables is set as:

$$\hat{Z} = h(\mathbf{X}) = [\hat{E}_0; \hat{E}_1; \hat{E}_2; \hat{E}_3; \hat{E}_4; \hat{E}_5; \hat{E}_6] \quad (11)$$

$$\mathbf{R}_G^i \hat{E}_i = \begin{bmatrix} 0 \\ 0 \\ 1 \end{bmatrix}, \quad (12)$$

$$\hat{E}_i = [\mathbf{R}_{G_{3,1}}^i \mathbf{R}_{G_{3,2}}^i \mathbf{R}_{G_{3,3}}^i]^{-T} \quad (13)$$

where:  $\mathbf{R}_G^i = \mathbf{R}_G^0 \mathbf{P}_0^1 \dots \mathbf{R}_{i-1}^i$  is determined from the D-H notation for individual joints based on  $\alpha_p, \theta_r$ .

For the presented manipulator, the measurement equations (8–13) are nonlinear. Since the measurement data from accelerometers are characterized by high noise, it is necessary to use a filter that limits the impact of noise on the accuracy of determining the position of the manipulator tip. An EKF [8, 9] can be used for this purpose, which also allows for the optimal data fusion from various sources. The described system is characterized by high data redundancy (21 measurement signals with 8 state variables).

The EKF is a two-phase recursive algorithm: in the first phase based on the state from the previous step  $\hat{X}_{k-1|k-1}$  is determined the estimated value of the current state  $\hat{X}_{k|k-1}$  from the moment  $k$  on the basis of measurements to the moment  $k-1$ .

$$\hat{X}_{k|k-1} = \mathbf{A} \hat{X}_{k-1|k-1} \quad (14)$$

For the presented arm with static measurements, the matrix  $\mathbf{A}$  relating the current state with the previous one is in the form of an identity matrix:  $\mathbf{A} = \mathbf{I}_{(8 \times 8)}$ , because it is rewritten from the previous state value (record was saved in (14) to keep the standard EKF appearance). As this is a static measurement, there are no drives that induce movement of the manipulator links. As a consequence, in the EKF prediction equation, the value associated with control vector in equation (14) is assumed to be zero.

The next step in the prediction phase is to determine the covariance matrix  $\mathbf{P}$  for the vector  $\hat{X}_{k|k-1}$  in the form:

$$\mathbf{P}_{k|k-1} = \mathbf{A} \mathbf{P}_{k-1|k-1} \mathbf{A}^T + \mathbf{Q}_{k-1} = \mathbf{P}_{k-1|k-1} \quad (15)$$

where:  $\mathbf{P}_{k-1|k-1}$  – covariance matrix  $\mathbf{P}$  at time  $k-1$ ;  $\mathbf{Q}_{k-1}$  – the process noise covariance matrix. It is assumed  $\mathbf{Q}_{k-1} = 0$  because the system is static and the process noise  $w_{k-1}$  has value 0.

Next, the second phase (correction stage) helps determine the measurement estimate for the state vector  $\hat{X}_k$  in the form:

$$\hat{Z}_k = \mathbf{h}(\hat{X}_k) \quad (16)$$

After calculating the expected value of the output vector, the residual of the measurement vector is determined in the form of the difference between the real measurement of and estimated on the basis of the model at time  $k$ :

$$r_k = Z_k - \hat{Z}_k \quad (17)$$

The covariance matrix of the estimate of the residual measurement vector is calculated from the formula:

$$\mathbf{S}_k = \mathbf{H} \mathbf{P}_{k|k-1} \mathbf{H}^T + \mathbf{R} \quad (18)$$

where the matrix  $\mathbf{H}$  is determined on the basis of partial derivatives of the output vector with respect to the state vector variables:

$$\mathbf{H} = \frac{\partial h}{\partial \mathbf{X}} \quad (19)$$

and  $\mathbf{R}$  is the covariance of the measurement noise covariance  $\mathbf{R} = \mathbf{I}_{(21 \times 21)} \sigma_{acc}^2$ , where  $\sigma_{acc}$  is the standard deviation of the accelerometer noise specified by the sensor manufacturer.

To determine how much the estimate should be corrected, to get closer to the actual state, we determine Kalman's gain in the form:

$$\mathbf{K}_k = \mathbf{P}_{k|k-1} \mathbf{H}_k^T \mathbf{S}_k^{-1} \quad (20)$$

using the individual components of the formula calculated in equations (15), (18), (19). In the last step of the correction phase, the corrected state vector and the corrected covariance matrix of the estimate are calculated in the form:

$$\hat{X}_{k|k} = \hat{X}_{k|k-1} + \mathbf{K}_k r_k \quad (21)$$

$$\mathbf{P}_{k|k} = (\mathbf{I} - \mathbf{K}_k \mathbf{H}_k) \mathbf{P}_{k|k-1} \quad (22)$$

The magnitudes determined in the equations (21) and (22) are then used as the input values for subsequent measurements carried out at time  $k+1$ .

The measurement stand (Fig. 2) consists of the measurement arm made using 3D printing technology and electronics mounted on the device in the form of a central module (32-bit microprocessor ARM Cortex-M3) with display and seven miniature circuit boards of the accelerometers mounted on other links of the arm. The software responsible for data logging and communication with the user has been written in [10]. The data obtained consisted of 30 measurements of the L position of the manipulator tip (Link 6) with respect to the base system (Link 0). The arm position was kept unchanged and the final data were analyzed in Excel.



Fig. 2. Measurement arm made in 3D printing technology

Each measurement consisted of accelerometer readings repeated 400 times and converted using the EKF. The EKF was initialized as described in [1]. The results of the position measurements are presented in Figs. 3, 4, 5 and the results of the orientation measurements are presented in Figs. 6, 7, 8. Both are in comparison with the results of estimation based on the average values described in [1].

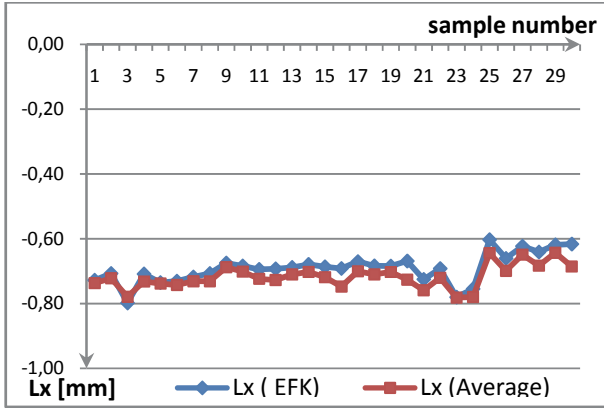


Fig. 3. Position measurements in  $L_x$  direction

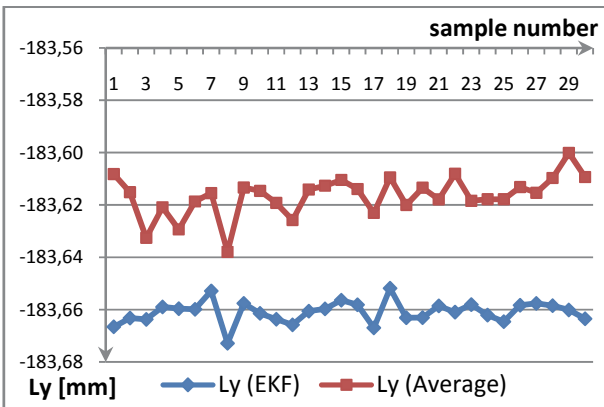


Fig. 4. Position measurements in  $L_y$  direction

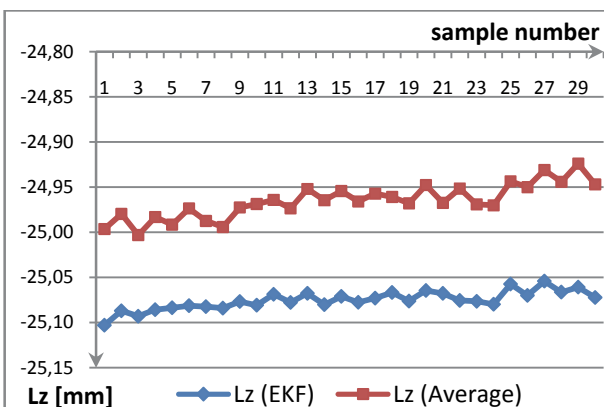


Fig. 5. Position measurements in  $L_z$  direction

Based on the position measurements, the standard deviations for position measurements using EKF were:  $\sigma_x = 0.04$  mm,  $\sigma_y = 0.004$  mm,  $\sigma_z = 0.01$  mm, while based on the calculated average the standard deviation values were:  $\sigma_x = 0.04$  mm,  $\sigma_y = 0.01$  mm,  $\sigma_z = 0.02$  mm.

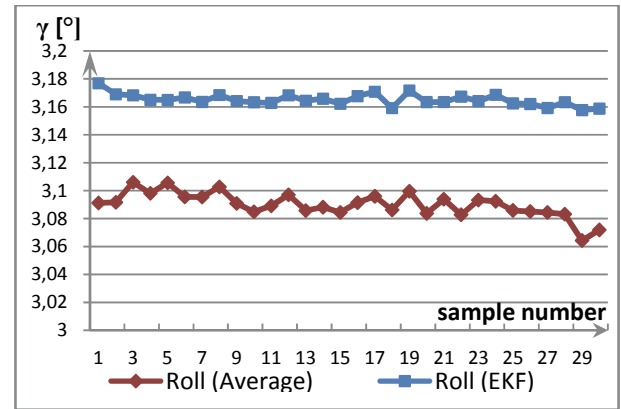


Fig. 6. Orientation measurements of  $\gamma$  angle (Roll)

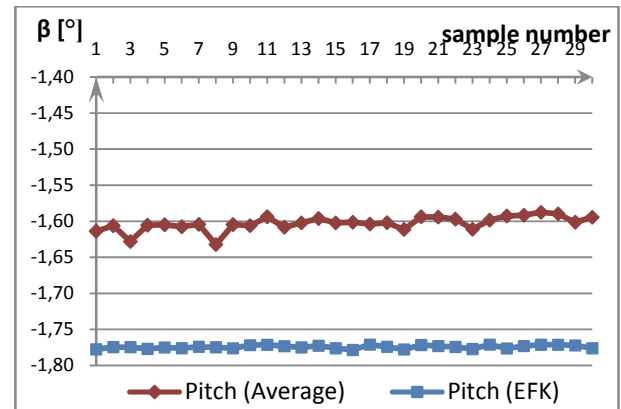


Fig. 7. Orientation measurements of  $\beta$  angle (Pitch)

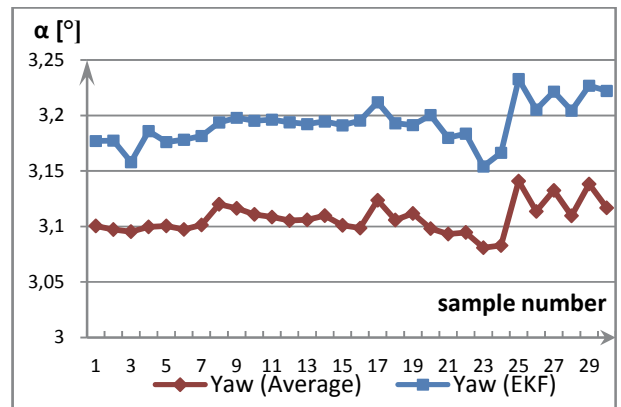


Fig. 8. Orientation measurements of  $\alpha$  angle (Yaw)

Based on the orientation measurements, the standard deviations for orientation measurements using EKF were:  $\sigma_\gamma = 0.004^\circ$ ,  $\sigma_\alpha = 0.018^\circ$ ,  $\sigma_\beta = 0.002^\circ$ . While for orientation measurements based on the calculated average the standard deviation values were:  $\sigma_\gamma = 0.009^\circ$ ,  $\sigma_\alpha = 0.014^\circ$ ,  $\sigma_\beta = 0.010^\circ$ .

### 3. Discussion

In the figures above, a significant difference can be observed between the mean values obtained using both methods. According to our analysis, the results obtained using EKF are more accurate as this method takes into account all measurement data for estab-

lishing a single state variable, while the conventional method, presented in [1], does not include all the measurement data.

Therefore, using EKF limits the effects of noise on the measurement and provides accurate results even with the static nature of the system.

#### 4. Conclusions

The presented prototype manipulator is used for determining the difference between the primary measurement before joint replacement and the secondary measurement after joint replacement; therefore, it is not important to determine the value of the L vector in the global system. Although the obtained results meet the requirements of these types of devices, the influence of factors such as deviation of the axis of the articulated joints from the vertical position, external forces, accuracy, and repeatability of arm fixing on markers is unknown. However, further work in this area will allow to estimate the total impact of all the factors associated with each link of the measurement arm.

#### AUTHORS

**Agnieszka Kobierska\*** – Lodz University of Technology, Institute of Machine Tools and Production Engineering, 1/15 B. Stefanowskiego Street, 90-924 Lodz, e-mail: agnieszka.kobierska@p.lodz.pl.

**Piotr Rakowski** – Lodz University of Technology, Institute of Machine Tools and Production Engineering, 1/15 B. Stefanowskiego Street, 90-924 Lodz, e-mail: piotr.rakowski@edu.p.lodz.pl.

**Leszek Podsędkowski** – Lodz University of Technology, Institute of Machine Tools and Production Engineering, 1/15 B. Stefanowskiego Street, 90-924 Lodz, e-mail: leszek.podsedkowski@p.lodz.pl.

\*Corresponding author

#### REFERENCES

- [1] P. Rakowski, A. Kobierska, L. Podsędkowski, and P. Poryzała, "Accuracy and Repeatability Tests on 6D Measurement Arm", *Mechanics and Mechanical Engineering*, vol. 21, no. 2, 2017, 425–436.
- [2] A. Kobierska, L. Podsędkowski, P. Rakowski, S. Rejmonczyk, J. Kaszowski, K. Olejniczak, B. Golasiński, and K. Kaczmarek, "A Methodology of Orthopaedic Measurement Arm Workspace Determination", *Mechanics and Mechanical Engineering*, vol. 21, no. 2, 2017, 185–191.
- [3] Peng Cheng and B. Oelmann, "Joint-Angle Measurement Using Accelerometers and Gyroscopes – A Survey", *IEEE Transactions on Instrumentation and Measurement*, vol. 59, no. 2, 2010, 404–414, 10.1109/TIM.2009.2024367.
- [4] M. El-Gohary and J. McNames, "Human Joint Angle Estimation with Inertial Sensors and Validation with A Robot Arm", *IEEE Transactions on Biomedical Engineering*, vol. 62, no. 7, 2015, 1759–1767, 10.1109/TBME.2015.2403368.
- [5] M. El-Gohary and J. McNames, "Shoulder and Elbow Joint Angle Tracking With Inertial Sensors", *IEEE Transactions on Biomedical Engineering*, vol. 59, no. 9, 2012, 2635–2641, 10.1109/TBME.2012.2208750.
- [6] E. Jezierski, *Dynamika Robotów (Robot Dynamics)*, Wydawnictwa Naukowo-Techniczne, 2006 (In Polish).
- [7] M. Quigley, R. Brewer, S. P. Soundararaj, V. Pradeep, Q. Le, and A. Y. Ng, "Low-cost accelerometers for robotic manipulator perception". In: *IEEE/RSJ International Conference on Intelligent Robots and Systems*, 2010, 6168–6174, 10.1109/IROS.2010.5649804.
- [8] R. Manish, "Linear and Non-linear Estimation Techniques: Theory and Comparison", 2014, arXiv:1406.5556.
- [9] P. Żak, "Master Manipulator Orientation Determination Method Using Extended Kalman Filter". In: *18th International Conference on Mechatronics – Mechatronika*, Brno, 2018, 276–280.
- [10] P. Poryzała, A. Kobierska, L. Podsędkowski, and P. Rakowski, "Prototyp urządzenia wspomagającego śródoperacyjną kontrolę długości kończyn dolnych podczas zabiegu endoprotezoplastyki stawu biodrowego (Prototype of a device for intraoperative measurements of limb length changes during total hip arthroplasty)", *Przegląd Elektrotechniczny*, vol. 93, no. 8, 2017, 129–132, 10.15199/48.2017.08.34.